Determination of Emission Factors of Pollutants from Biomass Burning of African fuels in Laboratory Measurements

Rudra P Pokhrel[1], Janica Gordon[1], Marc N. Fiddler[1], and Solomon Bililign[1]

[1]North Carolina A&T State University

November 24, 2022

Abstract

Biomass burning (BB) is a major source of pollutants that impact local, regional, and global climate, air quality, and public health. However, the influence of burning conditions and fuel type on emission factors of pollutants is still not well understood. Here, we present the results from a laboratory study of emission factors of pollutants from seven different sub-Saharan African biomass fuels combusted under a wide range of burning conditions ranging from smoldering to flaming. We found that particulate matter (PM) and CO emission factors (EF; g (kg wood)$^{-1}$) are highly sensitive to the burning conditions, with an order of magnitude variation between flaming and smoldering burning conditions. NO EF shows a fuel type dependence, with higher NO EF for fuels with larger nitrogen content. We observed a linear correlation between PM and CO EF and proposed that CO EF could be used as a proxy for estimating PM EF in cookstove emissions. The proposed relationship is valid regardless of the fuel type, moisture content, stove types, and origin of the fuel. Unlike total PM, EF of inorganic species do not show dependence on burning conditions. Finally, we showed that burning biomass fuels in a tube furnace would be an exceptional experimental approach to study BB emission under controlled burning conditions.

Determination of Emission Factors of Pollutants from Biomass Burning of African fuels in Laboratory Measurements

Rudra P. Pokhrel[1,4], Janica Gordon[2], Marc N. Fiddler[3,4], Solomon Bililign[1,2,4]

[1]Department of Physics, North Carolina A&T State University Greensboro, NC 27411

[2]Department of Applied Sciences and Technology, North Carolina A&T State University, Greensboro, NC 27411

[3]Department of Chemistry, North Carolina A&T State University, Greensboro, NC 27411

[4]ISET Center North Carolina A&T State University, Greensboro, NC 27411

Corresponding author: Solomon Bililign (bililign@ncat.edu)

Key Points:

- Particulate matter and CO emission factors are highly sensitive to the burning conditions of the fuel
- Emission factor of CO could be used as a proxy for estimating emission factor of particulate matter in cookstove emissions.
- Fuel nitrogen content plays a significant role in the emission factor of NO.

Abstract

Biomass burning (BB) is a major source of pollutants that impact local, regional, and global climate, air quality, and public health. However, the influence of burning conditions and fuel type on emission factors of pollutants is still not well understood. Here, we present the results from a laboratory study of emission factors of pollutants from seven different sub-Saharan African biomass fuels combusted under a wide range of burning conditions ranging from smoldering to flaming. We found that particulate matter (PM) and CO emission factors (EF; g (kg wood)$^{-1}$) are highly sensitive to the burning conditions, with an order of magnitude variation between flaming and smoldering burning conditions. NO EF shows a fuel type dependence, with higher NO EF for fuels with larger nitrogen content. We observed a linear correlation between PM and CO EF and proposed that CO EF could be used as a proxy for estimating PM EF in cookstove emissions. The proposed relationship is valid regardless of the fuel type, moisture content, stove types, and origin of the fuel. Unlike total PM, EF of inorganic species do not show dependence on burning conditions. Finally, we showed that burning biomass fuels in a tube furnace would be an exceptional experimental approach to study BB emission under controlled burning conditions.

1 Introduction

Biomass burning (BB), which includes open burning as well as cookstove emission (Akagi et al., 2011), emits gaseous and particulate pollutants that impact human health, including premature deaths and low birth weight. Emissions from BB are associated with a variety of acute respiratory illnesses such as asthma, chronic obstructive pulmonary disease, pulmonary fibrosis, pneumonia, and lung cancer (Delfino et al., 2009; Elliott et al., 2013; Henderson et al., 2011; Holstius et al., 2012; Johnston et al., 2011; Johnston et al., 2012; Naeher et al., 2007; Rappold et al., 2011; Smith and Pillarisetti, 2017; Stefanidou et al., 2008; Sutherland et al., 2005). Air pollution (ambient and household) is a major threat to human health, which increases the risk of pulmonary and cardiovascular diseases and contributes to an estimated premature death of 7 million people globally (Forouzanfar et al., 2016). BB is the largest source of primary carbonaceous particles and the second largest source of trace gases in the atmosphere (Andreae, 2019; Andreae and Merlet, 2001; Bond et al., 2004). The impacts of air pollution in Africa are significant, since Africa is the single largest source of BB emissions; accounting for more than half of global BB carbon emissions (Ichoku et al., 2016; Ichoku et al., 2008; Lamarque et al., 2010; Roberts et al., 2009; Roberts and Wooster, 2008; Schultz et al., 2008; van der Werf et al., 2010). Emissions from Africa are expected to grow due to a rapid increase in population. By 2100, the population of Africa is predicted to be 40% of the global population (UN, 2017). The sharp increase in population will increase the use of domestic and commercial combustion sources, since it is estimated that about 500 million people will remain without access to electricity by 2030 (IEA, 2020). In 2018, about 900 million people in sub-Saharan Africa relied on solid fuel and that demand is expected to grow sharply (IEA, 2020). Solid fuels such as wood, charcoal, animal dung, and crop residue are the main sources of energy in African households (Beyene and Koch, 2013). Besides health impacts, emissions from Africa will also impact the global climate. Black carbon (BC), which is only second to CO_2 in its climate warming contribution (Bond et al., 2013; Jacobson, 2001), is the main particulate emitted from BB. Up to 80% of the BC emissions from Africa were attributed to residential solid fuel burning (Bond et al., 2013).

Even though Africa is the single largest source of global BB carbon emission, studies focusing on African BB emission are recent and very limited (Eck et al., 2003; Flamant et al., 2018; Haywood et al., 2020; Redemann et al., 2020; Vakkari et al., 2014). Most of the global emission inventories available and used for Africa are based on emissions data from North America, Europe, and Asia (Bond et al., 2007; Bond et al., 2004; Klimont et al., 2009; Klimont et al., 2013; Lamarque et al., 2010; Streets et al., 2004). The use of such inventories for air quality and climate modeling studies in Africa resulted in large uncertainties (Assamoi and Liousse, 2010; Liousse et al., 2014; Liousse et al., 2010). The only way to reduce these uncertainties is to use emission factors derived from local measurements of African fuels in the emission inventories. There have been several field studies reporting cookstove emissions in Africa (Adkins et al., 2010; Beltramo and Levine, 2013; Coffey et al., 2017; Eilenberg et al., 2018; Jary et al., 2014; Johnson et al., 2011; Oluwole et al., 2013; Pennise et al., 2009; Rosa et al., 2014; Wathore et al., 2017) but most of the studies are limited to only a few air pollutants; mostly CO and particulate matter (PM) (Thomas et al., 2015). Besides this, the variabilities in estimated EFs are attributed to factors like stove type, fuel type, moisture content, fuel origin, etc. which makes direct comparison of the results difficult. Due to a lack of proper parameterization schemes, there is a significant uncertainty in the emission factors used in air quality and climate models.

In this study, we report the results of laboratory combustion experiments for studying the impact of combustion conditions on the emissions of gaseous and particulate air pollutants. African biomass samples representative of solid fuels used in sub-Saharan African households were combusted under various burning conditions. We quantified the impact of burning conditions by burning the same fuel under a variety of burning conditions and by burning different fuels under the same conditions and comparing the resulting emissions.

2 Materials and Methods

2.1 Sample Preparation and Burning Setup

Six different sub-Saharan African fuels with local names and scientific names listed in Table 1, and a native eastern North American fuel (white pine) were used for this study. African fuels were collected from Ethiopia and Botswana, whereas the North American fuel was collected locally in North Carolina. All the fuels were stored in a fume hood for drying and fuel moisture content was estimated before the experiments by measuring mass loss in the fuel due to overnight heating in the oven set at 90 ^{o}C, as in previous studies (Christian et al., 2003; Pokhrel et al., 2021). The estimated fuel moisture content in this study was below 10% for all fuels.

The elemental composition of the fuel was estimated by using a carbon, hydrogen, and nitrogen (CHN) analyzer (CHN analyzer 2400 series II, PerkinElmer, USA) that employs the Pregl-Dumas method. Each biomass sample was converted into fine dust using a saw then about 5 mgs of the fine powder was weighed on a tin capsule and crimped with tweezers. These capsule samples were placed inside the autosampler wheel and were introduced to a high temperature reactor where they were combusted in a temporarily oxygen enriched atmosphere. CO_2, H_2O, and nitrogen oxides produced during combustion were carried by helium gas and passed through a reduction tube where oxides of nitrogen were reduced to molecular nitrogen. Finally, the gases were homogeneously mixed as they passed through the mixing chamber and the components of the resulting gas mixture were chromatographically separated before being

quantified with a thermal conductivity detector. The percentages of elemental composition of carbon, hydrogen, and nitrogen in the fuel measured in this study are presented in Table 1. CHN measurements had a manufacturer-specified accuracy of < 0.3% and precision of < 0.2%.

Biomass combustion was conducted at North Carolina Agricultural and Technical State University (NCAT) indoor burning facility. Details of the burning facility and the experimental and chamber cleaning procedures are reported in our previous studies (Pokhrel et al., 2021; Smith et al., 2020a; Smith et al., 2020b; Smith et al., 2019) and only a brief description is provided here. The schematic of the NCAT burning facility and measurement set up is shown in Figure S1. Biomass combustion was performed in a tube furnace and the smoke was transported to the environmental chamber by mixing with zero air supplied to the tube furnace at constant flow rate (10 standard liters per minute). The furnace was disconnected from the chamber about 10 minutes after ignition and a constant flow of make-up gas (typically 4 L min^{-1} provided by zero air generator) was supplied to the chamber.

The temperature of the furnace can be set from room temperature to 1000 ^{o}C, but this study used combustion temperatures between 450 ^{o}C and 800 ^{o}C. A mixing fan located inside the chamber was turned on for about 15 to 20 minutes after combustion. The temperature and relative humidity (RH) inside the chamber were monitored using a hygrometer (Traceable Products, Model 4085; humidity range 5% to 95%). The typical temperature in the chamber during these experiments ranged from 21 °C – 24 °C and RH below 5%. Following each set of measurements, the chamber was flushed with zero air at a flow rate of 20 L min^{-1} until the particle mass reached below 2 µg m^{-3} and nitric oxide and ozone concentrations were below 5 ppbv.

Table 1: The elemental composition of biomass samples used in this work.

Local / Common Name	Scientific Name	Elemental Composition (%)		
		C	H	N
Girar / Umbrella thorn, Flat-top acacia	*Acacia abyssinica*	45.8	6.7	0.4
Bahir Zaf / Eucalyptus	*Eucalyptus camaldulensis*	46.1	6.6	0.3
Mopane / balsam tree	*Colophospermum mopane*	46.4	6.8	0.3
Mukusi / African teak	*Baikiaea plurijuga*	46.6	6.8	0.5
Woyira /Olive	*Olea europaea*	49.3	6.9	0.2
Wanza	*Cordia Africana*	45.5	6.5	0.5
White Pine	*Pinus strobus*	46.8	6.8	0.1

2.2 Instrumentation

We measured the different gas phase species emitted from biomass burning as described below. Carbon dioxide (CO_2) and carbon monoxide (CO) concentrations were measured using a CO_2 analyzer (model 41C Thermo Scientific) and a CO analyzer (model 48C Thermo Scientific), respectively. These monitors were calibrated before and after the experiments using certified standard gas cylinders (199.7 ppmv for CO and 5028 ppmv for CO_2 from Airgas National Welders). Nitrogen oxides (NO_x) were measured with a Monitor Labs fluorescence analyzer (model 8840). The NOx monitor was calibrated using a certified standard gas cylinder (53.12 ppmv for NO from Airgas National Welders). Due to a failure in the catalytic converter in the NOx monitor, we were only limited to NO measurements in this study. A UV photometric ozone (O_3) analyzer (model 49 Thermo Electron) was used to measure the O_3 concentrations. The O_3 analyzer was calibrated using a gas titration method (DeMore and Patapoff, 1976). Briefly, O_3 was produced by passing zero air through the generator having a UV lamp (11SC-1, Spectroline) and titrated with NO in a ~30 mL glass mixing ball. The reduction in the NO concentration was measured by the calibrated NOx monitor and O_3 concentration was measured based on the loss in the NO concentration.

We measured the particle size distribution in the range of 14 -720 nm using a Scanning Mobility Particle Sizer (SMPS, TSI). The SMPS consists of an electrostatic classifier (TSI, Model 3080), long Differential Mobility Analyzer (DMA, TSI, Model 3081), and a general-purpose water-based Condensation Particle Counter (WCPC, TSI, Model 3787). We also measured the size-selected particle effective density (ρeff) using an Aerosol Particle Mass analyzer (APM, Kanomax Inc., Model 3602) by connecting DMA and APM in series. Briefly, the DMA was used to select the aerosol size based on its electrical mobility and then the size-selected aerosol passed through the APM, which classified the aerosol based on its mass to charge ratio. The WCPC connected downstream of APM was used to measure the concentration of the particles at each mass. During this study, the APM was operated in stepping mode where the rotational speed of the APM was kept constant and the voltage underwent stepwise changes to produce a series of selected sizes to determine the particle mass distribution. Details of the operation principle of the APM can be found elsewhere (McMurry et al., 2002; Park et al., 2003; Park et al., 2004). Particle effective density is calculated using:

$$\rho_{eff} = \frac{6m_p}{\pi d_m{}^3} \qquad 1$$

where m_p is the particle mass and d_m is the mobility diameter.

An aerosol chemical speciation monitor (ACSM; Aerodyne Research Inc., USA) was used to measure submicron non-refractory particulate matter (NR-PM) including organics, nitrate, sulfate, ammonium, and chloride. Aerosol from the chamber was sampled into the ACSM through a critical orifice with a diameter of 100 μm at a constant flow rate of 85 mL min^{-1}. The ACSM was calibrated with ammonium nitrate and ammonium sulfate to estimate the ionization efficiency and relative ionization efficiencies. The recorded data were processed using the ACSM local toolkit (v. 1.6.0.3) for Igor Pro. Details about the ACSM can be found elsewhere (Ng et al., 2011).

169 2.3 Modified combustion efficiency and emission factor calculation

170 Emissions from fires can be impacted by many factors such as fuel geometry, moisture content,
171 and environmental variables (Stockwell et al., 2014). The relative amount of flaming and
172 smoldering combustion is quantified by calculating modified combustion efficiency (MCE) for
173 the fire.

174 $$\mathrm{MCE} = \frac{\Delta \mathrm{CO}_2}{\Delta \mathrm{CO}_2 + \Delta \mathrm{CO}} \quad (2)$$

175 where $\Delta \mathrm{CO}_2$, and $\Delta \mathrm{CO}$ are the background corrected CO_2 and CO concentrations,
176 respectively (Stockwell et al., 2014; Yokelson et al., 2009; Yokelson et al., 1997). Background
177 concentrations were measured before the ignition of each burn. Though higher MCE values are
178 attributed to more complete combustion, flaming and smoldering can happen simultaneously.
179 Typically, an MCE of ~ 0.8 is attributed to purely smoldering, an MCE of ~ 0.9 represents
180 roughly equal amounts of flaming and smoldering, and an MCE of ~ 0.99 is attributed to purely
181 flaming combustion (Stockwell et al., 2014). The reported MCE values represent a fire average;
182 integrated over all stages of combustion, since smoke was introduced into the chamber sampling
183 the entire burn and measurements from the chamber could not distinguish between different
184 stages. We adjusted the furnace temperature between 450 °C to 800 °C to achieve the different
185 burning conditions. During the lower temperature burning cases (450 °C to 500 °C) the
186 calculated MCE were below 0.9, whereas for the higher temperature burning cases (700°C and
187 800°C) the calculated MCE were at or above 0.95.

188 The emission factor (EF) is defined as the amount of pollutant released per unit mass of
189 the fuel burned. We calculated EFs using carbon mass balance approach; assuming all of the
190 carbon had been measured and all of the burned carbon was volatilized (Selimovic et al., 2018;
191 Stockwell et al., 2014; Yokelson et al., 2009; Yokelson et al., 1999):

192 $$\mathrm{EF(X)}\ (\mathrm{g\ kg^{-1}}) = F_c \times 1000 \times \frac{\mathrm{MW_X}}{\mathrm{MW_C}} \times \frac{\Delta \mathrm{X}}{\Delta \mathrm{CO} + \Delta \mathrm{CO}_2} \quad (3)$$

193 where F_c is the fuel carbon content; $\mathrm{MW_C}$ is the molecular weight of carbon; $\mathrm{MW_X}$ is the
194 molecular weight of species X; $\Delta \mathrm{CO}$, $\Delta \mathrm{CO}_2$, and $\Delta \mathrm{X}$ are the background corrected mixing ratios
195 of CO, CO_2, and species X. Due to limitations in our capability to measure non-CO_2 and non-CO
196 carbon emissions, we neglected the carbon emissions other than CO and CO_2 in the denominator
197 of the equation (3). This may lead to overestimation of EFs by a few percent (Akagi et al., 2011;
198 Andreae and Merlet, 2001). However, this source of error is negligible compared to other
199 sources of error, such as variations in burning conditions, moisture content, fuel type differences,
200 etc. The mass ratio of background corrected PM to the background corrected CO was multiplied
201 by the EF of CO to determine the EFs of PM (g kg^{-1}) (Stockwell et al., 2016). Similarly, total
202 particle number (PN) EFs (# kg^{-1}) is calculated by multiplying the ratio of PN to the CO mass
203 concentration by the EF of CO. Since number concentrations inside the chamber change rapidly
204 due to diffusional loss, coagulation, and gravitational settling, we corrected those losses based on
205 the first order decay rate of the total number concentration, as shown in Figure S2.

206 2.4 Particulate mass measurement

207 We converted the particle volume distribution measured by the SMPS to PM mass by
208 multiplying the particle volume with the effective density of the particle. In this study, the SMPS
209 sampled from 14-720 nm, so the PM mass estimated in this study would be ~PM1. In-software
210 multiple charging correction was applied. We found that ρ_{eff} was size independent for burns with

MCE < 0.9 (Pokhrel et al., 2021), so for burns with MCE < 0.9, we used the average value of ρ_{eff} calculated from 4-6 different sizes. For burns with MCE > 0.9, ρ_{eff} shows a size dependence, with smaller values of ρ_{eff} for larger mobility sizes. So, for MCE > 0.9 cases, we used the mass mobility exponent relationship to estimate the ρ_{eff} at a desired mobility diameter. The mass mobility exponent relation is expressed as a power-law relationship between m_p and d_m.

$$m_p = C d_m^{D_{fm}} \quad (4)$$

where C is a pre-factor and D_{fm} is the mass mobility exponent (Park et al., 2003; Park et al., 2004; Pokhrel et al., 2021). On combining Equations 1 and 4, ρeff can be expressed as:

$$\rho_{eff} = \frac{6 C d_m^{D_{fm}}}{\pi {d_m}^3} = C' d_m^{D_{fm}-3} \quad (5)$$

where $C' = \frac{6C}{\pi}$ is a constant. Based on Equation 4, we first estimated the mass mobility exponent and the pre-factor then applied those values in Equation 5 to estimate the ρ_{eff} at a particular size. We set the upper limit of ρ_{eff} as 2 g cm^{-3} (which is assigned as the density of primary particles) as in a previous study (Maricq and Xu, 2004). One representative example of ρeff calculated for a set of DMA midpoint diameters is shown in Figure S3 and the details of the mass estimation is explained in the supplementary information.

ACSM measurements were used to estimate the mass of NR-PM. A recent study (Lim et al., 2019) found that the aerosol mass spectrometer collection efficiency depends on the aerosol volatility, with collection efficiencies ranging from 0.35 to 0.64. So, the use of a constant collection efficiency would bias the estimated mass concentrations of NR-PM. In addition, due to a slight difference in size range measured by our SMPS (up to 720 nm) and ACSM (up to 1 μm) and a lack of black carbon mass measurements, we did not estimate the collection efficiency of the ACSM. We estimated the mass percentage of organic aerosol (OA), nitrate, sulfate, ammonium, and chloride in NR-PM and used that fraction to estimate the mass of each component based on SMPS mass measurements by assuming black carbon accounts for 5% of the total PM for smoldering-dominated fires. Since the fraction of BC mass in flaming dominated burns is highly variable, we did not estimate the NR-PM mass for those burns. The mass of NR-PM estimated this way might have some bias if the black carbon mass is more or less than 5% of the PM mass.

Table 2. Fuel based average modified combustion efficiency and emission factor (g kg^{-1}) of different fuels. Values inside the parentheses represent one standard deviation of the average.

Fuel	MCE	CO_2 EF	CO EF	NO EF
Acacia	0.88 (0.07)	1474 (114)	129 (72)	1.19 (0.70)
Eucalyptus	0.83 (0.09)	1408 (157)	179 (100)	0.72 (0.48)
Mopane	0.83 (0.11)	1415 (168)	183 (107)	0.98 (0.44)
Mukusi	0.87 (0.09)	1483 (156)	143 (99)	1.21 (0.53)
Olive	0.91 (0.07)	1637 (125)	109 (79)	0.703 (0.39)
Wanza	0.89 (0.05)	1487 (89)	114 (57)	1.89 (0.82)
White Pine	0.87 (0.07)	1497 (118)	140 (75)	0.67 (0.23)

3 Result and Discussion

3.1 Simulation of biomass burning at lab

Seven different fuels were burned under various burning conditions by adjusting the temperature of the furnace to simulate the different stages of the fire. The temperature of the furnace was adjusted between 450 °C to 800 °C in this study. The fuel burning condition was quantified by calculating the MCE of the burn, as discussed in section 2.3. Even though the MCE can be influenced by other factors other than furnace temperature, we generally found lower temperature combustion was smoldering-dominated and higher temperature combustion (> 700 °C) typically resulted in MCE > 0.95 that were flaming-dominated. Figure 1 shows the distribution of the MCE of the different burns in this study and a comparison with previous laboratory and field studies of open BB and cookstove emissions (Grieshop et al., 2017; Saliba et al., 2018; Selimovic et al., 2018; Stockwell et al., 2014). We compare the MCE values because the MCE shows a good correlation with emissions of different gaseous and particulate pollutants and is used extensively in emission factor measurement studies (Akagi et al., 2011; Bilsback et al., 2019; Champion et al., 2017; Christian et al., 2003; Liu et al., 2017; Selimovic et al., 2018; Stockwell et al., 2014; Yokelson et al., 2013; Yokelson et al., 2008; Yokelson et al., 1997). In comparing a few representative laboratory experiments and field studies, the MCE for the laboratory studies is skewed towards flaming conditions (MCE > 0.92 or above) as shown by a very narrow width of the violin plot below MCE = 0.9. As recommended in a recent review article (Hodshire et al., 2019), more laboratory studies of smoldering fires are needed to study the emission behavior under lower MCE conditions. Even though a field study of cookstove emissions shown in Figure 1 is dominated by high MCE, this is not always the case, as shown by a recent cookstove field study (Eilenberg et al., 2018). With this in mind, we designed experiments to conduct burns of biomass fuels for a wider and uniformly distributed range of MCE values, as shown in Figure 1. As indicated by the width of the violin plot, we were able to conduct burns of biomass fuels from a nearly purely smoldering to a nearly purely flaming condition in a more controlled way. As explained in more details under section 3.2, despite using seven different fuels, we were able to burn all the fuels within a similar range of MCE values. This fact suggests that conducting combustion studies of biomass fuels in a tube furnace could be an exceptional approach to study emissions from BB as a function of burning conditions.

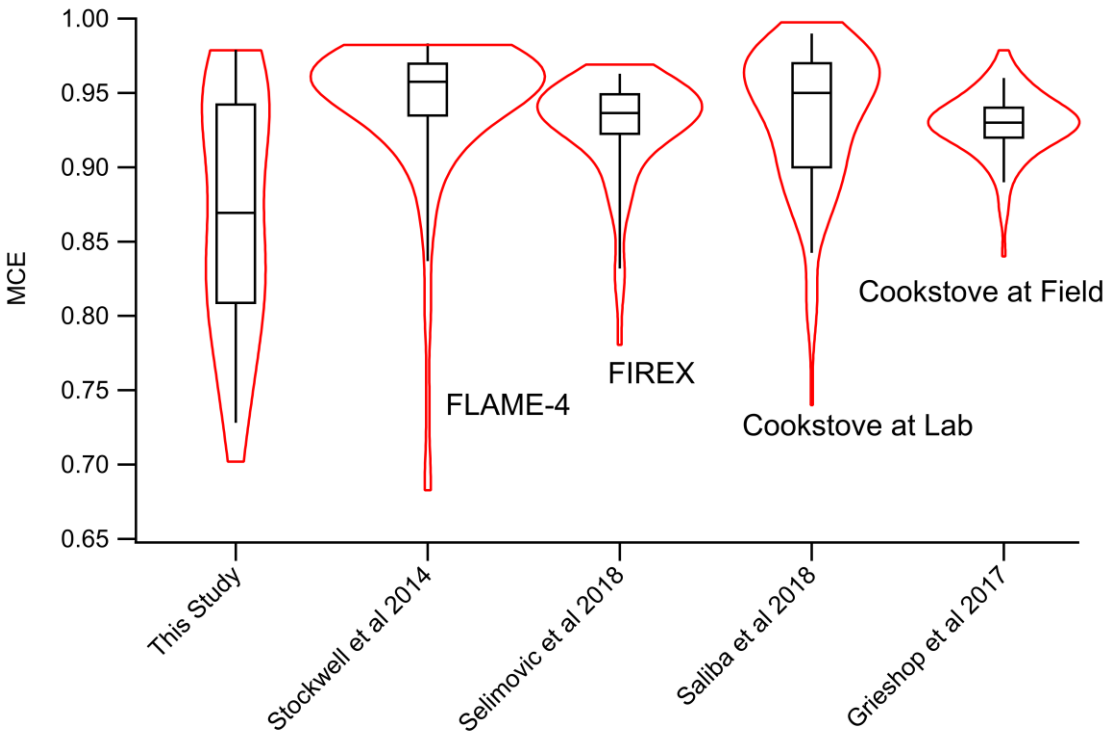

Figure 1. Violin plots showing comparison of MCE for previous laboratory and field studies of BB and cookstove emissions. Boxes represent the interquartile range with whiskers as the 95th and 5th percentile of the data and the line inside the box is the median. Violins (area enclosed by red lines) represent the kernel density to show the distribution of MCE.

3.2 Emission of gas-phase species

We conducted a total of 39 different burning experiments with at least 4 burns for each fuel type, as shown in the axis label of Figure 2. The distribution of the MCE for each fuel type is shown in Figure 2 (a). The MCE values observed in this study from all fuels were between 0.702 and 0.981 with an average value of 0.870 (0.080). The value inside the parenthesis represents one standard deviation about the average. These values are consistent with previous laboratory experiments for biomass burning (McMeeking et al., 2009; Selimovic et al., 2018; Stockwell et al., 2014) as well as for cookstove emissions (Bilsback et al., 2018; Saliba et al., 2018). For each fuel, the interquartile range of the MCE is slightly different but the average MCE for each fuel type lies within one standard deviation of the average for all fuels, as shown in Table 2. Like the MCE, we also observed a similar range of EFs of CO_2 and CO for all fuels, as shown in Figure 2 (b) and (c). Not surprisingly, EFs show a good correlation for CO_2 and anticorrelation for CO with the MCE values, as observed in a previous study (Selimovic et al., 2018). The estimated ranges of CO_2 EFs based on all burning experiments lies between 1196 g kg^{-1} to 1775 g kg^{-1} with an average value of 1484 (146) g kg^{-1} and that of CO lies between 21.39 g kg^{-1} to 323.09 g kg^{-1} with average value of 141.38 (86.98) g kg^{-1}. The values in parenthesis represent one standard deviation about the average. These values lie within the range of EFs of CO_2 and CO for open cooking found in a previous study (Akagi et al., 2011). The range of CO_2 and CO EFs based on each fuel type is shown in Table 2. Unlike CO_2, the emission factor of CO

is highly sensitive to the burning conditions, with an order of magnitude increase when changing the MCE value from ~0.75 to ~0.95 for the same fuel. This suggests that variations in CO EFs found in different cookstove types (Grieshop et al., 2017; Roden et al., 2006; Wathore et al., 2017) could potentially be due to differences in fuel burning efficiencies, which can be influenced by factors other than cookstove type (Stockwell et al., 2014). These could include fuel dryness, surface area, and fuel type. We compare our estimated values of CO_2 and CO EFs with previous laboratory studies (Selimovic et al., 2018; Stockwell et al., 2014) for a wide variety of fuels as well as a field study focusing on African BB emissions (Barker et al., 2020). In addition, we also compare the CO EFs with previous cookstove emission studies (Eilenberg et al., 2018; Grieshop et al., 2017). As shown in Figure S4 (a) & (b), our estimated values compare well with previous studies and show a similar correlation between MCE and EFs of CO_2 and CO.

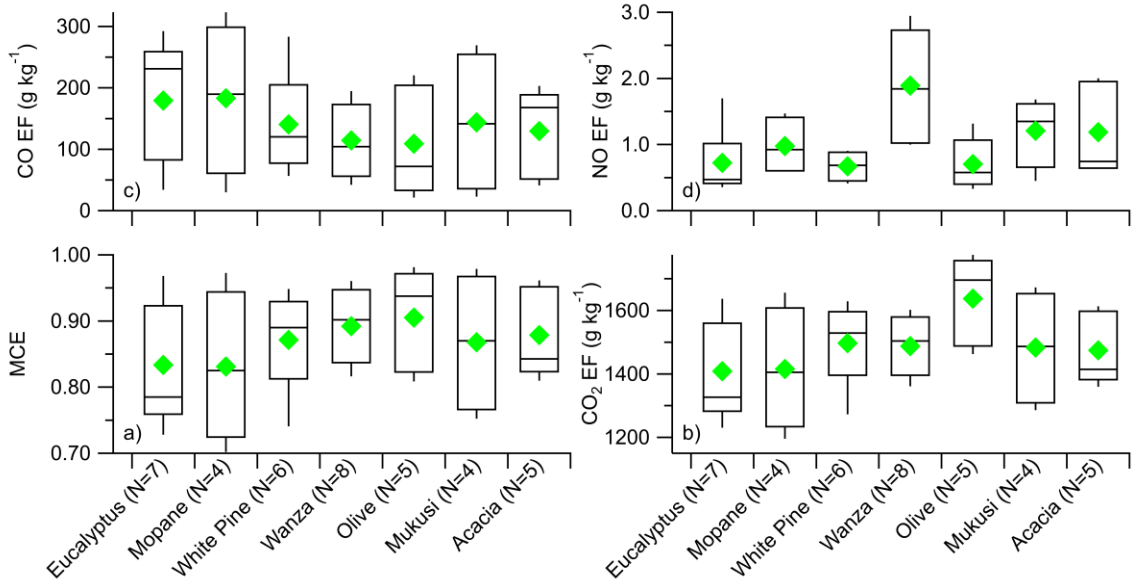

Figure 2. Box and whisker plots of a) MCE, b) emission factor of CO_2, c) emission factor of CO, and d) emission factor of NO for the different fuels listed on the bottom axis. Numbers inside the bracket on the bottom axis represent the number of burns for each fuel type. Boxes represent the interquartile range with whiskers as the 95th and 5th percentile of the data. The line inside the box is the median and the green diamonds are the mean of the data.

The range of NO EFs found in this study lie between 0.33 g kg^{-1} and 2.95 g kg^{-1} with an average value of 1.11 (0.71) g kg^{-1}, which compares well with the NO EF for open cooking (1.42 (0.42) g kg^{-1}) found in a previous study (Akagi et al., 2011). Like CO_2 and CO, we also compared the NO EFs with previous laboratory studies (Selimovic et al., 2018; Stockwell et al., 2014) and found NO EFs derived from African fuels are consistent with those from western US, as shown in Figure S4 (c). Like in previous studies, we did not observe a good correlation of NO EFs with the MCE. Unlike CO_2 and CO, NO EFs show a fuel type dependence, with some fuels showing consistently higher values than others. For a similar range of MCE, NO EFs for wanza is consistently higher than most of the other fuels, as shown in Table 2. As evident from Figure 2 (d), NO EFs for eucalyptus, white pine, and olive are relatively lower than the rest of the fuels, which aligns well with the relatively lower fuel nitrogen content of those fuels as shown in Table 1. This result is consistent with previous studies concluding that NO emission is dependent on

the fuel nitrogen content (Andreae and Merlet, 2001; McMeeking et al., 2009; Tihay-Felicelli et al., 2017). To further explore this, we performed a multiple regression of NO EFs as a function of MCE, fuel nitrogen content, and an independent term. Multiple regression analysis significantly improves the correlation with an r2 increase from 0.41 obtained from simple linear regression with respect to MCE to 0.70 with MCE and nitrogen content. This fact suggests that the incorporation of fuel nitrogen content can significantly improve the prediction of NO EFs and that MCE and nitrogen content accounts for 70% of the NO EF dependence. Details of the regression analysis is presented in the supplementary information. Furthermore, we also explored the impact of combustion condition on NO emission by burning the same fuel under various combustion conditions quantified by the MCE values. For the same fuel (wanza), the NO EF shows a good correlation with MCE value, with larger NO emissions for flaming condition and lower emissions for smoldering conditions. On changing the MCE from ~0.81 to ~0.96, the NO EF increased by the factor of 3, as shown in Figure S5. EFs of gas phase species for all burns are provided on Table S1.

3.3 Emission of particulate matter

Like EFs of CO, EFs of PM also show large variations, with estimated values ranging from 0.82 g kg^{-1} to 25.10 g kg^{-1} for different burning conditions. Given such a large variation in EFs (almost two orders in magnitude) and no obvious discrepancies between different fuel types, we parameterized PM EFs with MCE. PM EFs shows good correlation ($r^2 = 0.76$) with MCE (as shown in Figure S6) having larger PM emissions for smoldering fires and lower PM emissions for flaming fires. Typically, for flaming-dominated fires (MCE > 0.95) the estimated EFs of PM are less than 5 g kg^{-1}, indicating that efficient burning can significantly reduce PM emissions. We compare our results with previous laboratory and field studies (Eilenberg et al., 2018; Grieshop et al., 2017; Hosseini et al., 2013; Jayarathne et al., 2018) of cookstove and biomass burning emissions and found a consistent relationship. There is some scatter in the data where some data points fall outside the 95% confidence interval of the best fit line, particularly for MCE > 0.9, but in general, the proposed relationship shows promising results. The PM mass calculated in this study is ~PM_1 because the upper limit of the SMPS used in this work was 720 nm. Most of the data from previous studies presented in Figure S6 are from $PM_{2.5}$ but, for fresh BB emissions, these range of PM are used interchangeably (Akagi et al., 2011) because majority of the PM mass (80-90%) comes from the diameters less than 1 μm (Reid et al., 2005). From an air pollution perspective, the study of PM emission is one of the key components needed to understand the severity of the impact of air pollution. There have been numerous cookstove emission studies focused on emissions of PM and other gaseous pollutants, and the variabilities in the estimated PM EFs values are often attributed to the impacts of stove types, fuel moisture conditions or fuel types (Bilsback et al., 2019; Bilsback et al., 2018; Champion et al., 2017; Coffey et al., 2017; Corbin et al., 2015; de la Sota et al., 2017; Du et al., 2017; Eilenberg et al., 2018; Grieshop et al., 2017; Islam et al., 2021; Mitchell et al., 2019; Mutlu et al., 2016; Pandey et al., 2017; Roden et al., 2006; Wathore et al., 2017). Due to large variations in reported PM EFs without proper parameterization, there will still remain a challenge in representing those emissions in models.

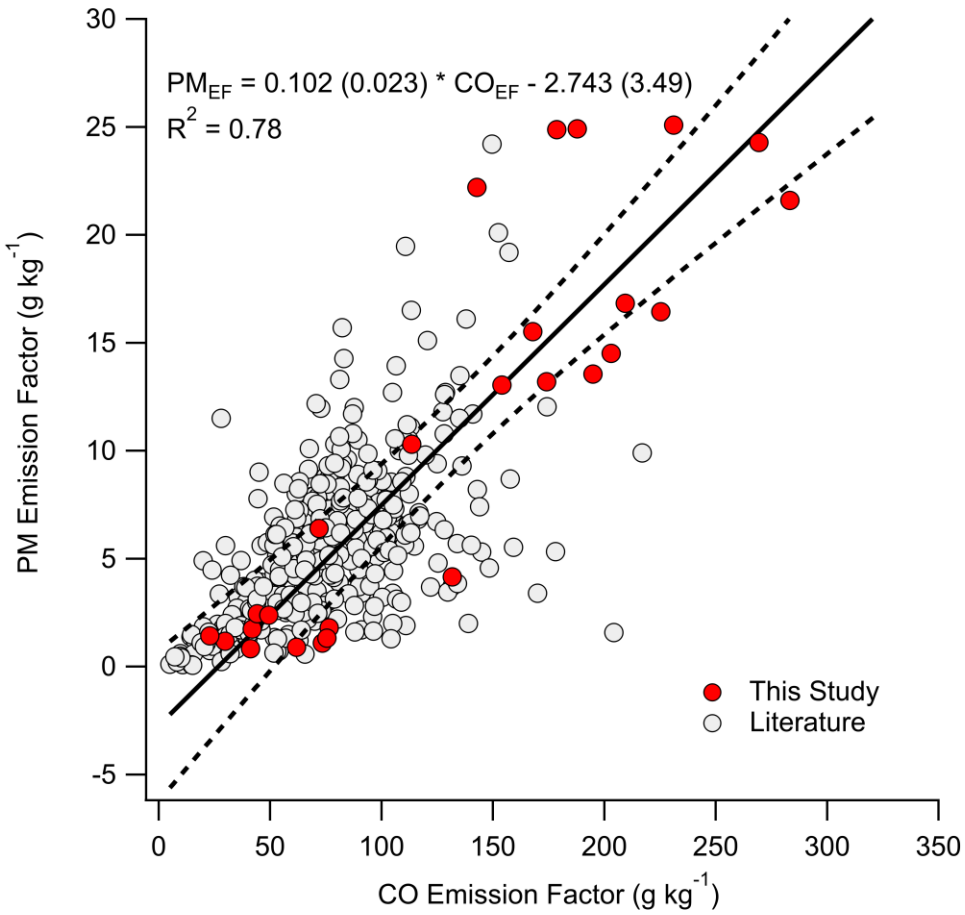

Figure 3. The particulate matter emission factor plotted as a function of CO emission factor. The solid black line is the linear best fit based on this study and the dotted black lines are the 95% confidence interval of the fit. Also included (gray filled circle) are the data from the previous studies. Original data and references for all the studies are provided in the supplementary information.

A recent review article on stove intervention programs in low- and middle-income countries found that there were more available measurements of CO than PM (Thomas et al., 2015). This could potentially be due to the fact that CO is substantially easier to measure with portable instruments compared to PM. There are a few studies which proposed a correlation between CO and PM EFs (Champion et al., 2017; Grieshop et al., 2017; Roden et al., 2009) but whether that relationship can still be applied for different stoves, fuels, and fuel moisture values is still uncertain. With that in mind, we parameterized EFs of PM as a function of EFs of CO based on this study. As shown in Figure 3, EFs of PM show a good positive correlation (r^2 =0.78) with EFs of CO from the data measured in this study. In addition, the slope of the regression (0.102 (0.023) g g^{-1}), which also represents the emission ratio of PM with CO, compares well with the 11-year average PM emission ratio with CO (0.109 (0.01) g g^{-1}) measured at Boise, ID (McClure and Jaffe, 2018) during a western US wildfire season. The intercept of the regression line is statistically insignificant (p value = 0.12) supporting the fact that for complete combustion (at CO = 0) there is no production of particulate matter. We compared the proposed regression based on this study with the data from previous studies. Data

from the literature includes 11 different studies (Coffey et al., 2017; Du et al., 2017; Eilenberg et al., 2018; Grieshop et al., 2017; Islam et al., 2021; Jetter et al., 2012; MacCarty et al., 2010; Mutlu et al., 2016; Roden et al., 2006; Roden et al., 2009; Wathore et al., 2017) with different fuels (dry and wet wood, dung, coconut shells, and biomass briquette); varieties of stoves types and 405 different field measurements from the south and east Asia, different parts of Africa, and laboratory studies (Table S2). As evident from Figure 3, regardless of all the aforementioned variabilities, the proposed regression based on this study captures the variabilities in the data. The majority of the literature data fall within the 95% confidence interval of the regression line, indicating that EFs of CO could be a good proxy for estimating EFs of PM for the cookstove using biomass fuel. Obviously, there is some scatter in the data which lies outside the 95% confidence interval ranges, but the majority (65%) lies within. We also examined the predictive capabilities of our proposed regression model. Based on the EFs of CO, we estimated the EFs of PM and found that predicted EFs of PM compared well with the measured literature values. The majority of the predicted EFs of PM lie close to the measured values as evident by highly dense data points around the one-to-one line, as shown in scatter density plot between predicted and measured EFs of PM (Figure S7). The mean bias error, mean absolute error, and root mean square error of the EF of PM are found to be 0.62 g kg^{-1}, 2.35 g kg^{-1}, and 3.24 g kg^{-1} respectively.

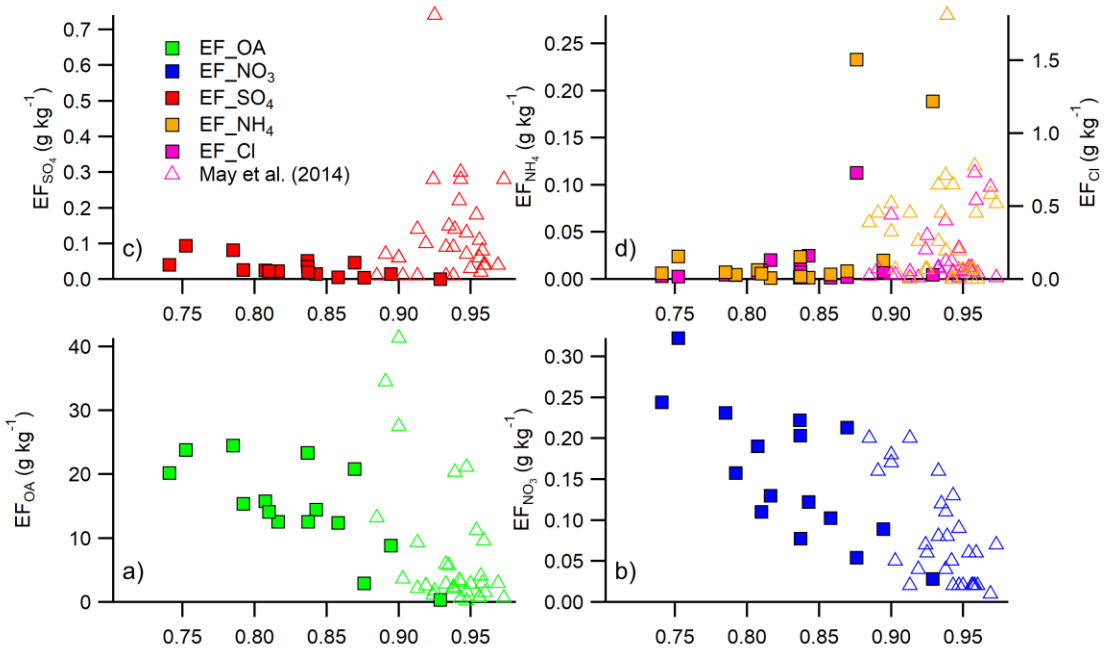

Figure 4. Emission factors of submicron aerosol species plotted as function of MCE for a) organic aerosol, b) nitrate, c) sulfate, and d) ammonium and chloride. Also included (open triangles) are the data from May et al. (2014) that is based on laboratory and airborne measurements.

Besides PM measured by the SMPS, we also reported the EFs of NR-PM measured by the ACSM. EFs of NR-PM as a function of MCE is shown in Figure 4, which also compares the NR-PM EFs from a previous study (May et al., 2014). As stated earlier in section 2.4, we only presented that data for smoldering fires (MCE ~0.9 and lower). OA is the major particulate

species emitted (>90% by mass in most of the burns) and has an order of magnitude higher EFs than the inorganic species. Such a high OA fraction has also been observed for smoldering fires in previous studies (Liu et al., 2017; May et al., 2014). The estimated average OA EF (15.33 ± 7.23 g kg^{-1}) is in good agreement with the previous study (May et al., 2014) which was measured during the prescribed montane fires (11.2 ± 2.7 g kg^{-1}). However, OA EFs in this study are significantly larger than chaparral and costal fire values measured by May et al. (2014); potentially due to the larger observed MCE during those fires. Similar to total PM, EFs of OA show a burning condition dependence with higher EF for the emissions with lower MCE. Besides OA, the dominant inorganic nonrefractory species measured by the ACSM includes sulfate, nitrate, ammonium, and chloride. The estimated average EFs of inorganic nonrefractory species are 0.032 (0.026), 0.16 (0.08), 0.034 (0.067), and 0.09 (0.175) g kg^{-1} for sulfate, nitrate, ammonium, and chloride respectively. Although these values are comparable with the previous study of fuels from the south east coastal plain (May et al., 2014), western US wildfires typically have larger values (Liu et al., 2017). This could potentially be due to fuel type dependence, as suggested in previous studies (Christian et al., 2003; Hosseini et al., 2013; May et al., 2014). Unlike OA, EFs of nonrefractory inorganic species (except nitrate) do not show dependence on burning conditions as quantified by the MCE except nitrate, which has also been observed in previous studies (May et al., 2014; McMeeking et al., 2009).

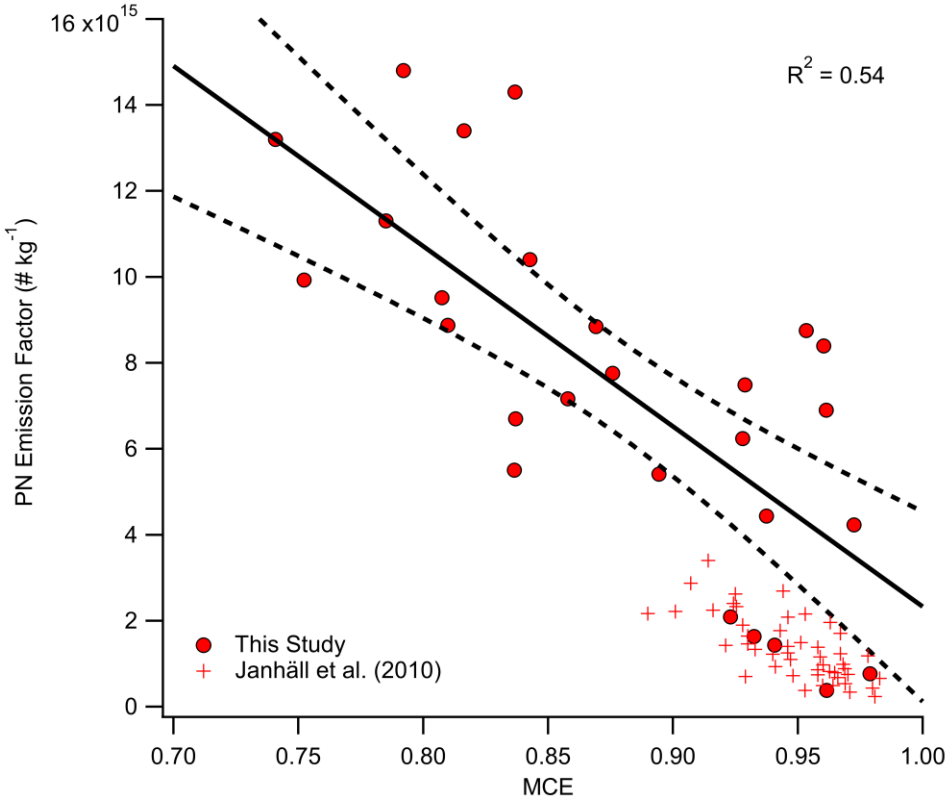

Figure 5. The particle number emission factor plotted as a function of MCE. Also included are the particle number emission factors from the previous study as shown in legend. The solid black line is the best linear fit of the data from this study and the dotted black lines are 95% confidence intervals of the fit.

Besides particle mass, we also estimated the emission factor of particle number emitted during combustion. Like PM EFs, PN EFs also show dependence on burning conditions with smoldering fire emitting an order of magnitude larger PN compared to flaming fires as shown in Figure 5. The range of PN EFs found in this study lies between 0.38 × 1015 kg^{-1} to 14.8 × 1015 kg^{-1} with an average value of 7.18 (4.16) × 1015 kg^{-1}. Unlike mass, the number emission factor only shows a reasonable correlation with MCE as quantified by the r^2 value of 0.54. All the EFs and MCE values for each burn are provided in Table S1. We compared our estimated values with a previous study (Janhäll et al., 2010) reporting PN EFs for different ambient fires and observed a decrease in PN EF with increasing MCE, while our values were consistently higher. This could potentially be due to the fact that aircraft measurements of ambient smoke might not sample fresh (t ~0 minute) smoke and may have sampled smaller particle sizes. Instruments used in their study were limited to particles greater than 100 nm in size. Our values are consistent with the previous laboratory study of different BB samples, with an estimated range of PN EFs between 2.88 (2.82) × 1015 kg^{-1} to 24.41 (22.85) × 1015 kg^{-1} (Bhattarai et al., 2018). The values inside the parentheses represent one standard deviation about the average.

4 Conclusions

We studied the emissions from seven different fuels (six African fuels and one eastern US native fuel) under a wide variety of burning conditions that range from purely smoldering to too close to purely flaming, as quantified by the resulting MCE values. We quantified the emission factors of trace gases (carbon dioxide, carbon monoxide, and nitric oxide), particulate mass and number as well as nonrefractory particulate matter constituents. The range of MCE observed in this study for all fuels lies between 0.702 to 0.981, with an average value of 0.870 (0.080). Regardless of fuel types and origin, the range of MCE values were similar for all fuels, resulting in similar CO and CO_2 EFs. The estimated ranges of CO_2 EFs based on all burning experiments lies between 1196 g kg^{-1} and 1775 g kg^{-1} with an average value of 1484 (146) g kg^{-1}. The CO EF range lies between 21.39 g kg^{-1} and 323.09 g kg^{-1} with an average value of 141.38 (86.98) g kg^{-1} . The range of NO EFs found in this study lies between 0.33 g kg^{-1} and 2.95 g kg^{-1} with an average value of 1.11 (0.71) g kg^{-1}, which shows a fuel type dependency with consistency higher EFs for fuels with higher nitrogen content. Even though NO EFs show a poor correlation with MCE, the incorporation of fuel nitrogen content in a multiple regression scheme significantly improves the correlation. The fit r^2 value goes from 0.41 to 0.70 upon inclusion of nitrogen content information, suggesting its incorporation can significantly improve the prediction of NO EFs. For the same fuel, emissions of NO show strong positive dependence on MCE (r^2 = 0.91) and NO EFs increase by a factor of 3 upon changing the MCE from ~0.81 to ~0.96. Although EFs of PM and OA show good correlation with MCE, nonrefractory inorganic species do not show a dependence on MCE. We found that the EF of PM is inversely correlated with MCE and changes by a factor of 30 between purely smoldering and purely flaming conditions (ranging from 0.82 g kg^{-1} to 25.10 g kg^{-1}). Our proposed regression between PM EFs and CO EFs shows a good consistency with 11 different cookstove emissions studies (Coffey et al., 2017; Du et al., 2017; Eilenberg et al., 2018; Grieshop et al., 2017; Islam et al., 2021; Jetter et al., 2012; MacCarty et al., 2010; Mutlu et al., 2016; Roden et al., 2006; Roden et al., 2009; Wathore et al., 2017) done in different parts of the globe; regardless of fuel types, moisture content, stove types, and fuel origin. Like PM mass, the PN EF also shows an MCE dependency, with smoldering fires emitting an order of magnitude higher PN EFs than flaming fires.

As pointed out by a recent review article (Hodshire et al., 2019), all the laboratory studies to date are skewed towards flaming fires which necessitates the study of more smoldering fires. Our combustion setup using a tube furnace allows us to have more control of burning conditions, with all the fuels burnt with a very similar range of MCE. As shown in Figure 1, the distribution of MCE in our study, ranging from 0.70 to 0.98, is more uniform and encompasses a greater variety of burning conditions than previous laboratory studies. This fact suggests that the burning of fuel in a tube furnace would be an exceptional experimental approach to study BB emission under controlled burning conditions.

Acknowledgments

We are thankful to Analytical Services Laboratory (ASL) of College of Agriculture and Environmental Sciences (CAES) at North Carolina Agriculture and Technical State University (NCAT) for the elemental analysis of wood samples. The authors are immensely grateful to Dr. Kiran Subedi for providing his expertise that greatly assisted the organic compositional analysis of our samples.

Funding

This work is supported by NSF Grant # AGS1831013. JG acknowledges the partial support by the Department of Education under the Title III HBGI grant. Any opinions, findings, and conclusions, or recommendations expressed in this material are those of the author(s) and do not necessarily reflect the views of the Department of Education.

References

Adkins, E., E. Tyler, J. Wang, D. Siriri, and V. Modi (2010), Field testing and survey evaluation of household biomass cookstoves in rural sub-Saharan Africa, *Energy for Sustainable Development*, *14*(3), 172-185, doi:https://doi.org/10.1016/j.esd.2010.07.003.

Akagi, S. K., R. J. Yokelson, C. Wiedinmyer, M. J. Alvarado, J. S. Reid, T. Karl, J. D. Crounse, and P. O. Wennberg (2011), Emission factors for open and domestic biomass burning for use in atmospheric models, *Atmos. Chem. Phys.*, *11*(9), 4039-4072, doi:10.5194/acp-11-4039-2011.

Andreae, M. O. (2019), Emission of trace gases and aerosols from biomass burning – an updated assessment, *Atmospheric Chemistry and Physics*, *19*(13), 8523-8546, doi:10.5194/acp-19-8523-2019.

Andreae, M. O., and P. Merlet (2001), Emission of trace gases and aerosols from biomass burning, *Global Biogeochemical Cycles*, *15*(4), 955-966, doi:10.1029/2000gb001382.

Assamoi, E.-M., and C. Liousse (2010), A new inventory for two-wheel vehicle emissions in West Africa for 2002, *Atmospheric Environment*, *44*(32), 3985-3996, doi:10.1016/j.atmosenv.2010.06.048.

Barker, P. A., et al. (2020), Airborne measurements of fire emission factors for African biomass burning sampled during the MOYA campaign, *Atmospheric Chemistry and Physics*, *20*(23), 15443-15459, doi:10.5194/acp-20-15443-2020.

Beltramo, T., and D. I. Levine (2013), The effect of solar ovens on fuel use, emissions and health: results from a randomised controlled trial, *Journal of Development Effectiveness*, *5*(2), 178-207, doi:10.1080/19439342.2013.775177.

Beyene, A. D., and S. F. Koch (2013), Clean fuel-saving technology adoption in urban Ethiopia, *Energy Economics*, *36*, 605-613, doi:10.1016/j.eneco.2012.11.003.

Bhattarai, C., V. Samburova, D. Sengupta, M. Iaukea-Lum, A. C. Watts, H. Moosmüller, and A. Y. Khlystov (2018), Physical and chemical characterization of aerosol in fresh and aged emissions from open combustion of biomass fuels, *Aerosol Science and Technology*, *52*(11), 1266-1282, doi:10.1080/02786826.2018.1498585.

Bilsback, K. R., et al. (2019), A Laboratory Assessment of 120 Air Pollutant Emissions from Biomass and Fossil Fuel Cookstoves, *Environ Sci Technol*, *53*(12), 7114-7125, doi:10.1021/acs.est.8b07019.

Bilsback, K. R., et al. (2018), The Firepower Sweep Test: A novel approach to cookstove laboratory testing, *Indoor Air*, *28*(6), 936-949, doi:10.1111/ina.12497.

Bond, T. C., E. Bhardwaj, R. Dong, R. Jogani, S. Jung, C. Roden, D. G. Streets, and N. M. Trautmann (2007), Historical emissions of black and organic carbon aerosol from energy-related combustion, 1850–2000, *Global Biogeochemical Cycles*, *21*(2), GB2018, doi:10.1029/2006GB002840.

Bond, T. C., et al. (2013), Bounding the role of black carbon in the climate system: A scientific assessment, *Journal of Geophysical Research: Atmospheres*, *118*(11), 5380-5552, doi:10.1002/jgrd.50171.

Bond, T. C., D. G. Streets, K. F. Yarber, S. M. Nelson, J.-H. Woo, and Z. Klimont (2004), A technology-based global inventory of black and organic carbon emissions from combustion, *Journal of Geophysical Research*, *109*, D14203, doi:10.1029/2003jd003697.

Champion, W. M., L. Connors, and L. D. Montoya (2017), Emission factors of fine particulate matter, organic and elemental carbon, carbon monoxide, and carbon dioxide for four solid fuels commonly used in residential heating by the U.S. Navajo Nation, *J Air Waste Manag Assoc*, *67*(9), 1020-1035, doi:10.1080/10962247.2017.1334717.

Christian, T. J., B. Kleiss, R. J. Yokelson, R. Holzinger, P. J. Crutzen, W. M. Hao, B. H. B. H. Saharjo, and D. E. Ward (2003), Comprehensive laboratory measurements of biomass-burning emissions: 1. Emissions from Indonesian, African, and other fuels, *Journal of Geophysical Research*, *108*(D23), 4719,, doi:10.1029/2003jd003704.

Coffey, E. R., D. Muvandimwe, Y. Hagar, C. Wiedinmyer, E. Kanyomse, R. Piedrahita, K. L. Dickinson, A. Oduro, and M. P. Hannigan (2017), New Emission Factors and Efficiencies from in-Field Measurements of Traditional and Improved Cookstoves and Their Potential Implications, *Environ Sci Technol*, *51*(21), 12508-12517, doi:10.1021/acs.est.7b02436.

Corbin, J. C., A. Keller, U. Lohmann, H. Burtscher, B. Sierau, and A. A. Mensah (2015), Organic Emissions from a Wood Stove and a Pellet Stove Before and After Simulated Atmospheric Aging, *Aerosol Science and Technology*, *49*(11), 1037-1050, doi:10.1080/02786826.2015.1079586.

de la Sota, C., M. Kane, J. Mazorra, J. Lumbreras, I. Youm, and M. Viana (2017), Intercomparison of methods to estimate black carbon emissions from cookstoves, *Sci Total Environ*, *595*, 886-893, doi:10.1016/j.scitotenv.2017.03.247.

Delfino, R. J., et al. (2009), The relationship of respiratory and cardiovascular hospital admissions to the southern California wildfires of 2003, *Occupational and Environmental Medicine*, *66*(3), 189-197, doi:10.1136/oem.2008.041376.

DeMore, W. B., and M. Patapoff (1976), Comparison of Ozone Determinations by Ultraviolet Photometry and Gas-Phase Titration, *Environmental Science & Technology*, *10*, 897-899.

Du, W., et al. (2017), Comparison of air pollutant emissions and household air quality in rural homes using improved wood and coal stoves, *Atmospheric Environment*, *166*, 215-223, doi:10.1016/j.atmosenv.2017.07.029.

Eck, T. F., et al. (2003), Variability of biomass burning aerosol optical characteristics in southern Africa during the SAFARI 2000 dry season campaign and a comparison of single scattering albedo estimates from radiometric measurements, *Journal of Geophysical Research: Atmospheres*, *108*(D13), n/a-n/a, doi:10.1029/2002jd002321.

Eilenberg, S. R., et al. (2018), Field measurements of solid-fuel cookstove emissions from uncontrolled cooking in China, Honduras, Uganda, and India, *Atmospheric Environment*, *190*, 116-125, doi:10.1016/j.atmosenv.2018.06.041.

Elliott, C. T., S. B. Henderson, and V. Wan (2013), Time series analysis of fine particulate matter and asthma reliever dispensations in populations affected by forest fires, *Environmental Health*, *12*(1), 11, doi:10.1186/1476-069X-12-11.

Flamant, C., et al. (2018), The Dynamics–Aerosol–Chemistry–Cloud Interactions in West Africa Field Campaign: Overview and Research Highlights, *Bulletin of the American Meteorological Society*, *99*(1), 83-104, doi:10.1175/bams-d-16-0256.1.

Forouzanfar, M. H., et al. (2016), Global, regional, and national comparative risk assessment of 79 behavioural, environmental and occupational, and metabolic risks or clusters of risks, 1990–2015: a systematic analysis for the Global Burden of Disease Study 2015, *The lancet*, *388*(10053), 1659-1724.

Grieshop, A. P., G. Jain, K. Sethuraman, and J. D. Marshall (2017), Emission factors of health- and climate-relevant pollutants measured in home during a carbon-finance-approved cookstove intervention in rural India, *Geohealth*, *1*(5), 222-236, doi:10.1002/2017GH000066.

Haywood, J. M., et al. (2020), Overview: The CLoud-Aerosol-Radiation Interaction and Forcing: Year2017 (CLARIFY-2017) measurement campaign, *Atmospheric Chemistry & Physics*, doi:10.5194/acp-2020-729.

Henderson, S. B., M. Brauer, Y. C. MacNab, and S. M. Kennedy (2011), Three Measures of Forest Fire Smoke Exposure and Their Associations with Respiratory and Cardiovascular Health Outcomes in a Population-Based Cohort, *Environmental Health Perspectives*, *119*(9), 1266-1271, doi:doi:10.1289/ehp.1002288.

Hodshire, A. L., et al. (2019), Aging Effects on Biomass Burning Aerosol Mass and Composition: A Critical Review of Field and Laboratory Studies, *Environ Sci Technol*, *53*(17), 10007-10022, doi:10.1021/acs.est.9b02588.

Holstius, D. M., C. E. Reid, B. M. Jesdale, and R. Morello-Frosch (2012), Birth Weight following Pregnancy during the 2003 Southern California Wildfires, *Environmental Health Perspectives*, *120*(9), 1340-1345, doi:doi:10.1289/ehp.1104515.

Hosseini, S., et al. (2013), Laboratory characterization of PM emissions from combustion of wildland biomass fuels, *Journal of Geophysical Research: Atmospheres*, *118*(17), 9914-9929, doi:10.1002/jgrd.50481.

Ichoku, C., et al. (2016), Biomass burning, land-cover change, and the hydrological cycle in Northern sub-Saharan Africa, *Environmental Research Letters*, *11*(9), doi:10.1088/1748-9326/11/9/095005.

Ichoku, C., L. Giglio, M. J. Wooster, and L. A. Remer (2008), Global characterization of biomass-burning patterns using satellite measurements of fire radiative energy, *Remote Sensing of Environment*, *112*(6), 2950-2962, doi:https://doi.org/10.1016/j.rse.2008.02.009.

IEA (2020), IEA, IRENA, UNSD, World Bank, WHO. 2020. Tracking SDG 7: The Energy Progress Report. World Bank, Washington DC. © World Bank. License: Creative Commons Attribution—NonCommercial 3.0 IGO (CC BY-NC 3.0 IGO).

Islam, M. M., R. Wathore, H. Zerriffi, J. D. Marshall, R. Bailis, and A. P. Grieshop (2021), In-use emissions from biomass and LPG stoves measured during a large, multi-year cookstove intervention study in rural India, *Sci Total Environ*, *758*, 143698, doi:10.1016/j.scitotenv.2020.143698.

Jacobson, M. Z. (2001), Global direct radiative forcing due to multicomponent anthropogenic and natural aerosols, *Journal of Geophysical Research: Atmospheres*, *106*(D2), 1551-1568, doi:doi:10.1029/2000JD900514.

Janhäll, S., M. O. Andreae, and U. Pöschl (2010), Biomass burning aerosol emissions from vegetation fires: particle number and mass emission factors and size distributions, *Atmospheric Chemistry & Physics*, *10*(3), 1427–1439, doi:https://doi.org/10.5194/acp-10-1427-2010.

Jary, H. R., J. Kachidiku, H. Banda, M. Kapanga, J. V. Doyle, E. Banda, C. Fox, S. B. Gordon, and K. Mortimer (2014), Feasibility of conducting a randomised controlled trial of a cookstove intervention in rural Malawi, *Int J Tuberc Lung Dis*, *18*(2), 240-247, doi:10.5588/ijtld.13.0485.

Jayarathne, T., et al. (2018), Nepal Ambient Monitoring and Source Testing Experiment (NAMaSTE): emissions of particulate matter from wood- and dung-fueled cooking fires, garbage and crop residue burning, brick kilns, and other sources, *Atmospheric Chemistry and Physics*, *18*(3), 2259-2286, doi:10.5194/acp-18-2259-2018.

Jetter, J., Y. Zhao, K. R. Smith, B. Khan, T. Yelverton, P. Decarlo, and M. D. Hays (2012), Pollutant emissions and energy efficiency under controlled conditions for household biomass cookstoves and implications for metrics useful in setting international test standards, *Environ Sci Technol*, *46*(19), 10827-10834, doi:10.1021/es301693f.

Johnson, M., N. Lam, D. Pennise, D. Charron, T. Bond, V. Modi, and J. Ndemere (2011), In-home emissions of greenhouse pollutants from rocket and traditional biomass cooking stoves in Uganda, *Washington: US Agency for International Development*.

Johnston, F., I. Hanigan, S. Henderson, G. Morgan, and D. Bowman (2011), Extreme air pollution events from bushfires and dust storms and their association with mortality in Sydney, Australia 1994–2007, *Environmental Research*, *111*(6), 811-816, doi:https://doi.org/10.1016/j.envres.2011.05.007.

Johnston, F. H., S. B. Henderson, Y. Chen, J. T. Randerson, M. Marlier, R. S. DeFries, P. Kinney, D. M. J. S. Bowman, and M. Brauer (2012), Estimated Global Mortality Attributable to Smoke from Landscape Fires, *Environmental Health Perspectives*, *120*(5), 695-701, doi:doi:10.1289/ehp.1104422.

Klimont, Z., et al. (2009), Projections of SO2, NOx and carbonaceous aerosols emissions in Asia, *Tellus B*, *61*(4), 602-617, doi:10.1111/j.1600-0889.2009.00428.x.

Klimont, Z., S. J. Smith, and J. Cofala (2013), The last decade of global anthropogenic sulfur dioxide: 2000–2011 emissions, *Environmental Research Letters*, *8*(1), 014003.

Lamarque, J. F., et al. (2010), Historical (1850–2000) gridded anthropogenic and biomass burning emissions of reactive gases and aerosols: methodology and application, *Atmos. Chem. Phys.*, *10*(15), 7017-7039, doi:10.5194/acp-10-7017-2010.

Lim, C. Y., D. H. Hagan, M. M. Coggon, A. R. Koss, K. Sekimoto, J. de Gouw, C. Warneke, C. D. Cappa, and J. H. Kroll (2019), Secondary organic aerosol formation from the laboratory oxidation of biomass burning emissions, *Atmospheric Chemistry and Physics*, *19*(19), 12797-12809, doi:10.5194/acp-19-12797-2019.

Liousse, C., E. Assamoi, P. Criqui, C. Granier, and R. Rosset (2014), Explosive growth in African combustion emissions from 2005 to 2030, *Environmental Research Letters*, *9*, 035003, doi:doi:10.1088/1748-9326/9/3/035003.

Liousse, C., et al. (2010), Updated African biomass burning emission inventories in the framework of the AMMA-IDAF program, with an evaluation of combustion aerosols, *Atmos. Chem. Phys.*, *10*(19), 9631-9646, doi:10.5194/acp-10-9631-2010.

Liu, X., et al. (2017), Airborne measurements of western U.S. wildfire emissions: Comparison with prescribed burning and air quality implications, *Journal of Geophysical Research: Atmospheres*, *122*(11), 6108-6129, doi:10.1002/2016jd026315.

MacCarty, N., D. Still, and D. Ogle (2010), Fuel use and emissions performance of fifty cooking stoves in the laboratory and related benchmarks of performance, *Energy for Sustainable Development*, *14*(3), 161-171, doi:10.1016/j.esd.2010.06.002.

Maricq, M. M., and N. Xu (2004), The effective density and fractal dimension of soot particles from premixed flames and motor vehicle exhaust, *Journal of Aerosol Science*, *35*(10), 1251-1274, doi:10.1016/j.jaerosci.2004.05.002.

May, A. A., et al. (2014), Aerosol emissions from prescribed fires in the United States: A synthesis of laboratory and aircraft measurements, *Journal of Geophysical Research: Atmospheres*, *119*(20), 11,826-811,849, doi:10.1002/2014jd021848.

McClure, C. D., and D. A. Jaffe (2018), Investigation of high ozone events due to wildfire smoke in an urban area, *Atmospheric Environment*, *194*, 146-157, doi:10.1016/j.atmosenv.2018.09.021.

McMeeking, G. R., et al. (2009), Emissions of trace gases and aerosols during the open combustion of biomass in the laboratory, *Journal of Geophysical Research*, *114*(D19), doi:10.1029/2009jd011836.

McMurry, P. H., X. Wang, K. Park, and K. Ehara (2002), The Relationship between Mass and Mobility for Atmospheric Particles: A New Technique for Measuring Particle Density, *Aerosol Science and Technology*, *36*(2), 227-238, doi:10.1080/027868202753504083.

Mitchell, E. J. S., Y. Ting, J. Allan, A. R. Lea-Langton, D. V. Spracklen, G. McFiggans, H. Coe, M. N. Routledge, A. Williams, and J. M. Jones (2019), Pollutant Emissions from Improved Cookstoves of the Type Used in Sub-Saharan Africa, *Combustion Science and Technology*, *192*(8), 1582-1602, doi:10.1080/00102202.2019.1614922.

Mutlu, E., et al. (2016), Mutagenicity and Pollutant Emission Factors of Solid-Fuel Cookstoves: Comparison with Other Combustion Sources, *Environ Health Perspect*, *124*(7), 974-982, doi:10.1289/ehp.1509852.

Naeher, L. P., M. Brauer, M. Lipsett, J. T. Zelikoff, C. D. Simpson, J. Q. Koenig, and K. R. Smith (2007), Woodsmoke Health Effects: A Review, *Inhalation Toxicology*, *19*(1), 67-106, doi:10.1080/08958370600985875.

Ng, N. L., et al. (2011), An Aerosol Chemical Speciation Monitor (ACSM) for Routine Monitoring of the Composition and Mass Concentrations of Ambient Aerosol, *Aerosol Science and Technology*, *45*(7), 780-794, doi:10.1080/02786826.2011.560211.

Oluwole, O., G. R. Ana, G. O. Arinola, T. Wiskel, A. G. Falusi, D. Huo, O. I. Olopade, and C. O. Olopade (2013), Effect of stove intervention on household air pollution and the respiratory health of women and children in rural Nigeria, *Air Quality, Atmosphere & Health*, *6*(3), 553-561, doi:10.1007/s11869-013-0196-9.

Pandey, A., S. Patel, S. Pervez, S. Tiwari, G. Yadama, J. C. Chow, J. G. Watson, P. Biswas, and R. K. Chakrabarty (2017), Aerosol emissions factors from traditional biomass cookstoves in India: insights from field measurements, *Atmospheric Chemistry and Physics*, *17*(22), 13721-13729, doi:10.5194/acp-17-13721-2017.

Park, K., F. Cao, D. B. Kittelson, and P. H. McMurry (2003), Relationship between particle mass and mobility for diesel exhaust particles, *Environ Sci Technol*, *37*(3), 577-583, doi:10.1021/es025960v.

Park, K., D. B. Kittelson, and P. H. McMurry (2004), Structural Properties of Diesel Exhaust Particles Measured by Transmission Electron Microscopy (TEM): Relationships to Particle Mass and Mobility, *Aerosol Science and Technology*, *38*(9), 881-889, doi:10.1080/027868290505189.

Pennise, D., S. Brant, S. M. Agbeve, W. Quaye, F. Mengesha, W. Tadele, and T. Wofchuck (2009), Indoor air quality impacts of an improved wood stove in Ghana and an ethanol stove in Ethiopia, *Energy for Sustainable Development*, *13*(2), 71-76, doi:https://doi.org/10.1016/j.esd.2009.04.003.

Pokhrel, R. P., J. Gordon, M. N. Fiddler, and S. Bililign (2021), Impact of combustion conditions on physical and morphological properties of biomass burning aerosol, *Aerosol Science and Technology*, *55*(1), 80-91, doi:10.1080/02786826.2020.1822512.

Rappold, A. G., et al. (2011), Peat Bog Wildfire Smoke Exposure in Rural North Carolina Is Associated with Cardiopulmonary Emergency Department Visits Assessed through Syndromic Surveillance, *Environmental Health Perspectives*, *119*(10), 1415-1420, doi:doi:10.1289/ehp.1003206.

Redemann, J., et al. (2020), An overview of the ORACLES (ObseRvations of Aerosols above CLouds and their intEractionS) project: aerosol-cloud-radiation interactions in the Southeast Atlantic basin, *Atmospheric Chemistry & Physics*, doi:10.5194/acp-2020-449.

Reid, J. S., R. Koppmann, T. F. Eck, and D. P. Eleuterio (2005), A review of biomass burning emissions part II: intensive physical properties of biomass burning particles, *Atmospheric Chemistry and Physics*, *5*, 799-825.

Roberts, G., M. J. Wooster, and E. Lagoudakis (2009), Annual and diurnal african biomass burning temporal dynamics, *Biogeosciences*, *6*(5), 849-866, doi:10.5194/bg-6-849-2009.

Roberts, G. J., and M. J. Wooster (2008), Fire Detection and Fire Characterization Over Africa Using Meteosat SEVIRI, *IEEE Transactions on Geoscience and Remote Sensing*, *46*(4), 1200-1218, doi:10.1109/TGRS.2008.915751.

Roden, C. A., T. C. Bond, S. Conway, and A. B. Osorto Pinel (2006), Emission Factors and Real-Time Optical Properties of Particles Emitted from Traditional Wood Burning Cookstoves, *Environmental Science & Technology*, *40*, 6750-6757.

Roden, C. A., T. C. Bond, S. Conway, A. B. Osorto Pinel, N. MacCarty, and D. Still (2009), Laboratory and field investigations of particulate and carbon monoxide emissions from traditional and improved cookstoves, *Atmospheric Environment*, *43*(6), 1170-1181, doi:10.1016/j.atmosenv.2008.05.041.

Rosa, G., F. Majorin, S. Boisson, C. Barstow, M. Johnson, M. Kirby, F. Ngabo, E. Thomas, and T. Clasen (2014), Assessing the Impact of Water Filters and Improved Cook Stoves on Drinking Water Quality and Household Air Pollution: A Randomised Controlled Trial in Rwanda, *PLOS ONE*, *9*(3), e91011, doi:10.1371/journal.pone.0091011.

Saliba, G., R. Subramanian, K. Bilsback, C. L'Orange, J. Volckens, M. Johnson, and A. L. Robinson (2018), Aerosol Optical Properties and Climate Implications of Emissions from Traditional and Improved Cookstoves, *Environ Sci Technol*, *52*(22), 13647-13656, doi:10.1021/acs.est.8b05434.

Schultz, M. G., A. Heil, J. J. Hoelzemann, A. Spessa, K. Thonicke, J. G. Goldammer, A. C. Held, J. M. C. Pereira, and M. van het Bolscher (2008), Global wildland fire emissions from 1960 to 2000, *Global Biogeochemical Cycles*, *22*(2), GB2002, doi:10.1029/2007GB003031.

Selimovic, V., R. J. Yokelson, C. Warneke, J. M. Roberts, J. de Gouw, J. Reardon, and D. W. T. Griffith (2018), Aerosol optical properties and trace gas emissions by PAX and OP-FTIR for laboratory-simulated western US wildfires during FIREX, *Atmospheric Chemistry and Physics*, *18*(4), 2929-2948, doi:10.5194/acp-18-2929-2018.

764 Smith, D. M., T. Cui, M. N. Fiddler, R. P. Pokhrel, J. D. Surratt, and S. Bililign (2020a),
765 Laboratory studies of fresh and aged biomass burning aerosol emitted from east African
766 biomass fuels – Part 2: Chemical properties and characterization, *Atmospheric Chemistry*
767 *and Physics*, *20*(17), 10169-10191, doi:10.5194/acp-20-10169-2020.

768 Smith, D. M., M. N. Fiddler, R. P. Pokhrel, and S. Bililign (2020b), Laboratory studies of fresh
769 and aged biomass burning aerosol emitted from east African biomass fuels – Part 1:
770 Optical properties, *Atmospheric Chemistry and Physics*, *20*(17), 10149-10168,
771 doi:10.5194/acp-20-10149-2020.

772 Smith, D. M., M. N. Fiddler, K. G. Sexton, and S. Bililign (2019), Construction and
773 Characterization of an Indoor Smog Chamber for Measuring the Optical and
774 Physicochemical Properties of Aging Biomass Burning Aerosols, *Aerosol and Air*
775 *Quality Research*, *19*(3), 467-483, doi:10.4209/aaqr.2018.06.0243.

776 Smith, K. R., and A. Pillarisetti (2017), Household Air Pollution from Solid Cookfuels and Its
777 Effects on Health., in *Injury Prevention and Environmental Health. 3rd edition*, edited by
778 M. CN, Nugent R and K. O, The International Bank for Reconstruction and Development
779 / The World Bank;, Washington (DC), doi:doi: 10.1596/978-1-4648-0522-6.

780 Stefanidou, M., S. Athanaselis, and C. Spiliopoulou (2008), Health Impacts of Fire Smoke
781 Inhalation, *Inhalation Toxicology*, *20*(8), 761-766, doi:10.1080/08958370801975311.

782 Stockwell, C. E., et al. (2016), Field measurements of trace gases and aerosols emitted by peat
783 fires in Central Kalimantan, Indonesia, during the 2015 El Niño, *Atmospheric Chemistry*
784 *and Physics*, *16*(18), 11711-11732, doi:10.5194/acp-16-11711-2016.

785 Stockwell, C. E., R. J. Yokelson, S. M. Kreidenweis, A. L. Robinson, P. J. DeMott, R. C.
786 Sullivan, J. Reardon, K. C. Ryan, D. W. T. Griffith, and L. Stevens (2014), Trace gas
787 emissions from combustion of peat, crop residue, domestic biofuels, grasses, and other
788 fuels: configuration and Fourier transform infrared (FTIR) component of the fourth Fire
789 Lab at Missoula Experiment (FLAME-4), *Atmospheric Chemistry and Physics*, *14*(18),
790 9727-9754, doi:10.5194/acp-14-9727-2014.

791 Streets, D. G., T. C. Bond, T. Lee, and C. Jang (2004), On the future of carbonaceous aerosol
792 emissions, *Journal of Geophysical Research: Atmospheres*, *109*(D24), n/a-n/a,
793 doi:10.1029/2004JD004902.

794 Sutherland, E. R., B. J. Make, S. Vedal, L. Zhang, S. J. Dutton, J. R. Murphy, and P. E. Silkoff
795 (2005), Wildfire smoke and respiratory symptoms in patients with chronic obstructive
796 pulmonary disease, *Journal of Allergy and Clinical Immunology*, *115*(2), 420-422,
797 doi:10.1016/j.jaci.2004.11.030.

798 Thomas, E., K. Wickramasinghe, S. Mendis, N. Roberts, and C. Foster (2015), Improved stove
799 interventions to reduce household air pollution in low and middle income countries: a
800 descriptive systematic review, *BMC Public Health*, *15*, 650, doi:10.1186/s12889-015-
801 2024-7.

802 Tihay-Felicelli, V., P. A. Santoni, G. Gerandi, and T. Barboni (2017), Smoke emissions due to
803 burning of green waste in the Mediterranean area: Influence of fuel moisture content and
804 fuel mass, *Atmospheric Environment*, *159*, 92-106, doi:10.1016/j.atmosenv.2017.04.002.

UN (2017), United Nations, Department of Economic and Social Affairs, Population Division (2017). World Population Prospects: The 2017 Revision, Key Findings and Advance Tables. Working Paper No. ESA/P/WP/248.

Vakkari, V., et al. (2014), Rapid changes in biomass burning aerosols by atmospheric oxidation, *Geophysical Research Letters*, *41*(7), 2644-2651, doi:10.1002/2014gl059396.

van der Werf, G. R., J. T. Randerson, L. Giglio, G. J. Collatz, M. Mu, P. S. Kasibhatla, D. C. Morton, R. S. DeFries, Y. Jin, and T. T. van Leeuwen (2010), Global fire emissions and the contribution of deforestation, savanna, forest, agricultural, and peat fires (1997–2009), *Atmos. Chem. Phys.*, *10*(23), 11707-11735, doi:10.5194/acp-10-11707-2010.

Wathore, R., K. Mortimer, and A. P. Grieshop (2017), In-Use Emissions and Estimated Impacts of Traditional, Natural- and Forced-Draft Cookstoves in Rural Malawi, *Environ Sci Technol*, *51*(3), 1929-1938, doi:10.1021/acs.est.6b05557.

Yokelson, R. J., et al. (2013), Coupling field and laboratory measurements to estimate the emission factors of identified and unidentified trace gases for prescribed fires, *Atmos. Chem. Phys.*, *13*(1), 89-116, doi:10.5194/acp-13-89-2013.

Yokelson, R. J., T. J. Christian, T. G. Karl, and A. Guenther (2008), The tropical forest and fire emissions experiment: laboratory fire measurements and synthesis of campaign data, *Atmospheric Chemistry & Physics*, *8*(13), 3509–3527, doi:https://doi.org/10.5194/acp-8-3509-2008.

Yokelson, R. J., et al. (2009), Emissions from biomass burning in the Yucatan, *Atmospheric Chemistry and Physics*, *9*, 5785–5812, doi:10.5194/acp-9-5788-2009

Yokelson, R. J., J. G. Goode, D. E. Ward, R. A. Susott, R. E. Babbitt, D. D. Wade, I. Bertschi, D. W. T. Griffith, and W. M. Hao (1999), Emissions of formaldehyde, acetic acid, methanol, and other trace gases from biomass fires in North Carolina measured by airborne Fourier transform infrared spectroscopy, *Journal of Geophysical Research: Atmospheres*, *104*(D23), 30109-30125, doi:10.1029/1999JD900817.

Yokelson, R. J., R. A. Susott, D. E. Ward, J. Reardon, and D. W. T. Griffith (1997), Emissions from smoldering combustion of biomass measured by open-path Fourier transform infrared spectroscopy, *Journal of Geophysical Research*, *102*(D15), 18,865-818,877.

Journal of Geophysical Research: Atmosphere

Supporting Information for

Determination of Emission Factors of Pollutants from Biomass Burning of African fuels in Laboratory Measurements

Rudra P. Pokhrel[1,4], Janica Gordon[2], Marc N. Fiddler[3,4], Solomon Bililign[1,2,4]

[1]Department of Physics, North Carolina A&T State University Greensboro, NC 27411

[2]Department of Applied Sciences and Technology, North Carolina A&T State University, Greensboro, NC 27411

[3]Department of Chemistry, North Carolina A&T State University, Greensboro, NC 27411

[4]ISET Center North Carolina A&T State University, Greensboro, NC 27411

Contents of this file

S1. Particle mass measurement

For smoldering-dominated burns, the effective density of the particle is independent of size (Pokhrel et al., 2021), so we used a constant density for all the mobility diameters in the SMPS. We estimated the total mass (M) by using the equation:

$$M = \int_{D_1}^{D_2} \frac{\pi}{6} D^3 \frac{dN}{d(\log D)}\, d(\log D)\, \rho_{eff} \quad (1)$$

Whereas for flaming-dominated burns, particle effective density is size dependent (Pokhrel et al. 2021). We used the mass mobility exponent relationship ($m_p = C d_m^{D_{fm}}$) to estimate the pre-factor (C) and mass mobility exponent (D_{fm}). We applied these values in the following equation

$$\rho_{eff} = \frac{6 C d_m^{D_{fm}}}{\pi {d_m}^3} \quad (2)$$

to estimate the effective density at desired mobility diameter in the SMPS. We set the upper limit of ρ_{eff} at 2 g cm-3 (which is assigned as the density of the primary particles), as was done in a previous study (Maricq and Xu, 2004) and shown in Figure S3. Thus, the effective density determined for each mobility diameter of SMPS is used to estimate the total mass using the equation:

$$M = \int_{D_1}^{D_2} \frac{\pi}{6} D^3 \frac{dN}{d(\log D)}\, d(\log D)\, \rho_{eff}(D) \quad (3)$$

S2. Regression analysis

To explore the dependence of NO EFs on burning condition and fuel nitrogen content, we perform simple linear regression of NO EFs with modified combustion efficiency (MCE) as:

$$EFNO = k0 + k1\ MCE \quad (4)$$

Based on the above equation, we found fitting coefficient as

k0 = -3.67 (±1.97), k1 = 5.49 (±2.26), and r2 = 0.41. The values inside the parenthesis represent the 95% confidence interval of the fitting coefficients.

In addition, we also performed the multiple regression analysis of NO EFs with MCE and fuel nitrogen content as:

$$EFNO = k0 + k1\ MCE + k2\ Nitrogen\ content \quad (5)$$

Based on equation 5, we found the following fitting coefficients with the 95% confidence interval presented as a number inside the parenthesis.

k0 = -4.28 (±1.44), k1 = 5.21 (±1.63), k2 = 2.51 (±0.89), and r2 = 0.70.

S3. Statistical analysis

To analyze the performance of proposed regression model of EF of PM as a function of EF of CO, we estimated following error as:

Mean Bias Error (MBE) = $\frac{1}{n}\sum_{i=1}^{n}(Predicted\ EF\ of\ PM - Measured\ EF\ of\ PM)$

Mean Absolute Error (MAE) = $\frac{1}{n}\sum_{i=1}^{n}|(Predicted\ EF\ of\ PM - Measured\ EF\ of\ PM)|$

Root Mean Square Error (RMSE) = $\sqrt{\frac{1}{n}\sum_{i=1}^{n}(Predicted\ EF\ of\ PM - Measured\ EF\ of\ PM)^2}$

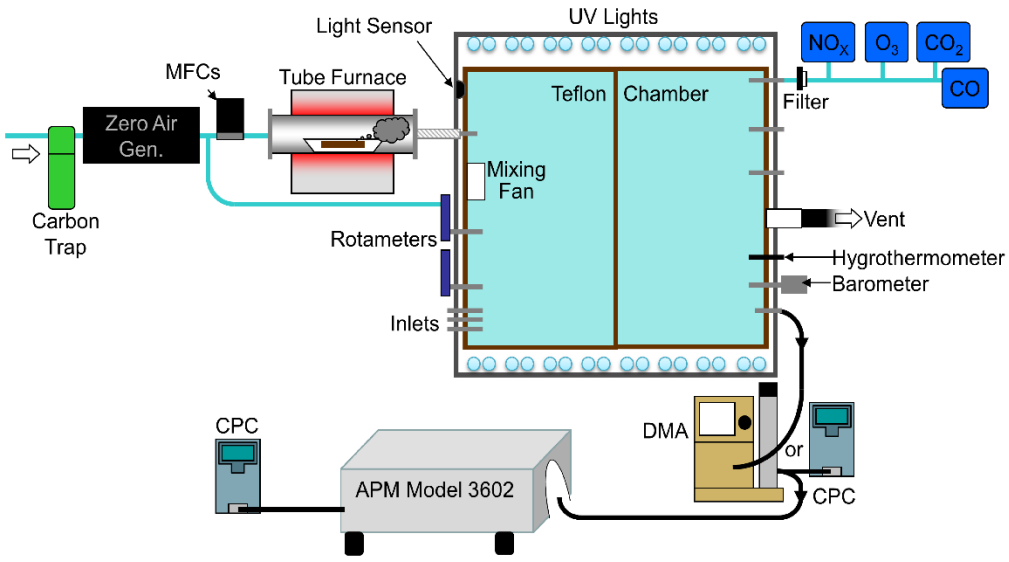

Figure S1. Schematic of NCAT biomass burning facility and measurement setup used in this study.

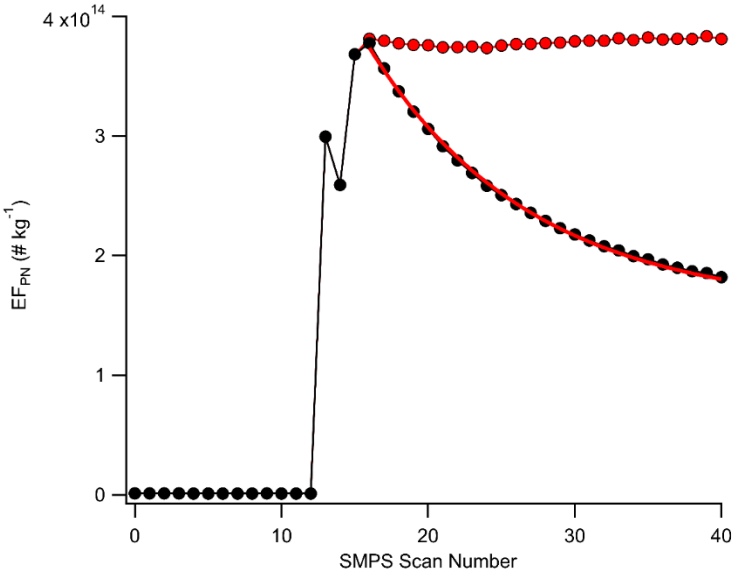

Figure S2. Particle loss adjustment inside the chamber. The black circles and the line represent the total particle emission factor without the loss correction in particles kg^{-1}, the solid red line represents the loss rate based on first order decay, and the red circle markers and line represent the loss-corrected total particle emission factor.

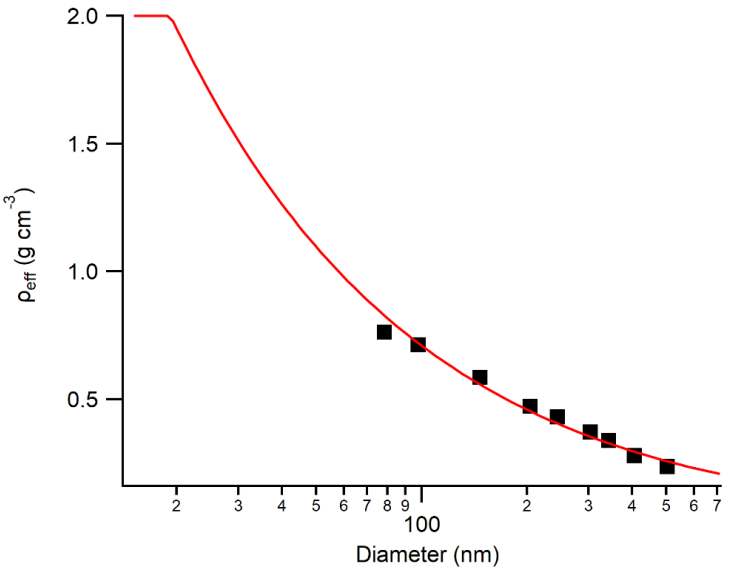

Figure S3. Particle effective density plotted as a function of mobility diameter for a burn with an MCE of 0.960. Black squares are the calculated effective densities using the APM and DMA, and the red line is the predicted effective density based on the mass mobility exponent and pre-factor using Equation 5 in the main text.

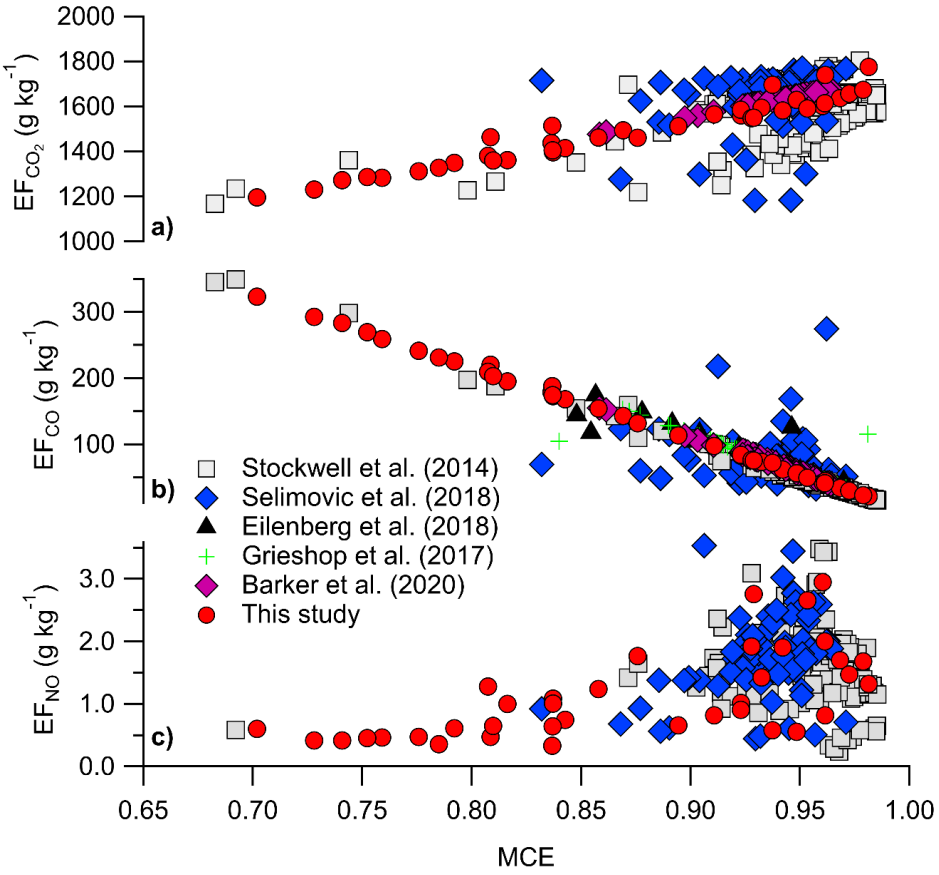

Figure S4. Emission factors of a) CO2, b) CO, and c) NO plotted as a function of MCE. Also included are the emission factors from previous laboratory (Selimovic et al., 2018; Stockwell et al., 2014), field (Barker et al., 2020), and cookstove (Eilenberg et al., 2018; Grieshop et al., 2017) studies that are indicated in legend.

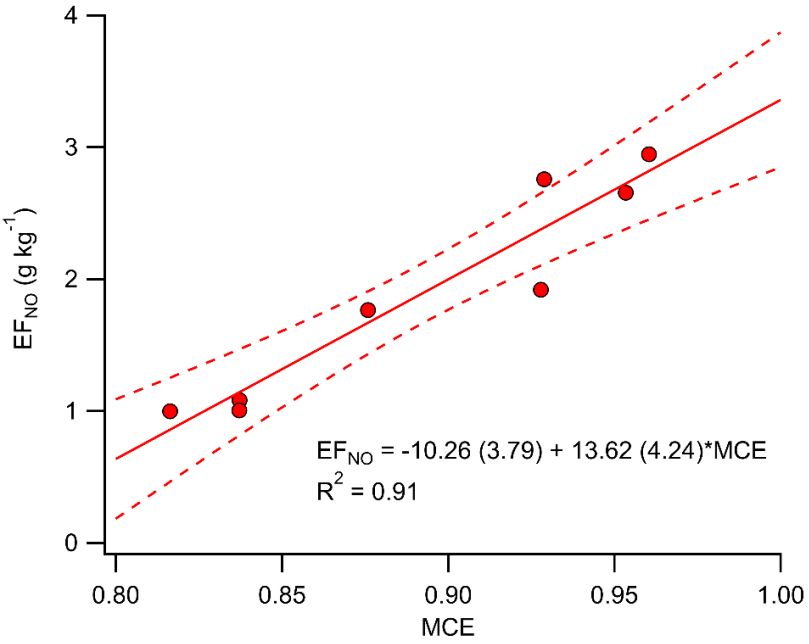

Figure S5. EF of NO as a function of MCE for wanza. The red solid line represents the best liner fit of the data and dotted red lines are the 95% confidence interval of the fitting line.

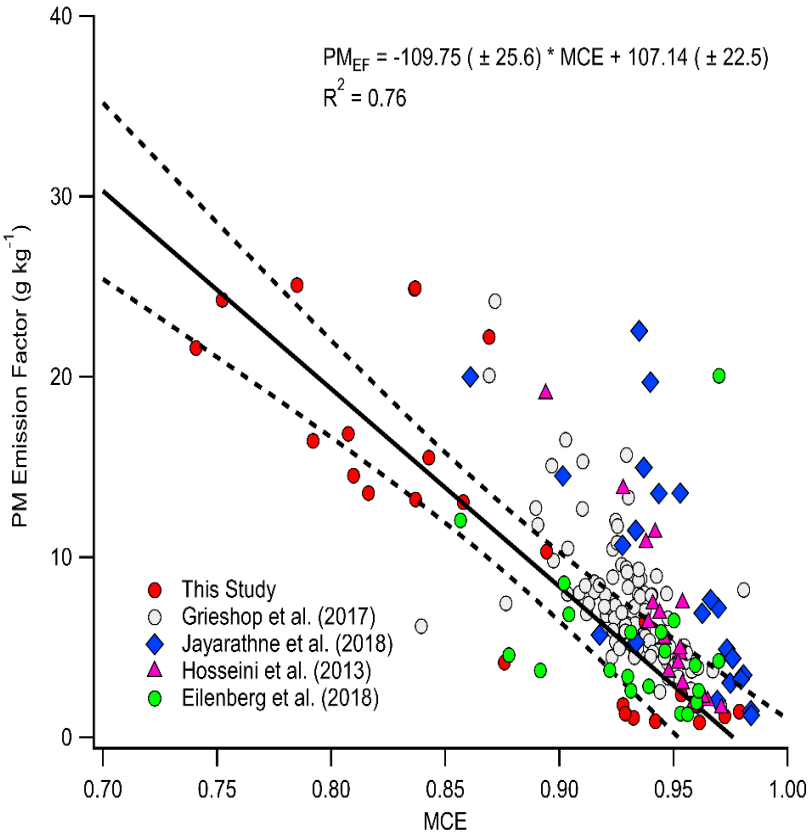

Figure S6. EFs of PM plotted as a function of MCE. The solid black line is the best linear fit of the data from this study and the dotted black lines are 95% confidence interval of the fit. Also included are the EFs of PM from the previous laboratory and field studies of cookstove and biomass burning emissions, as shown in the legend.

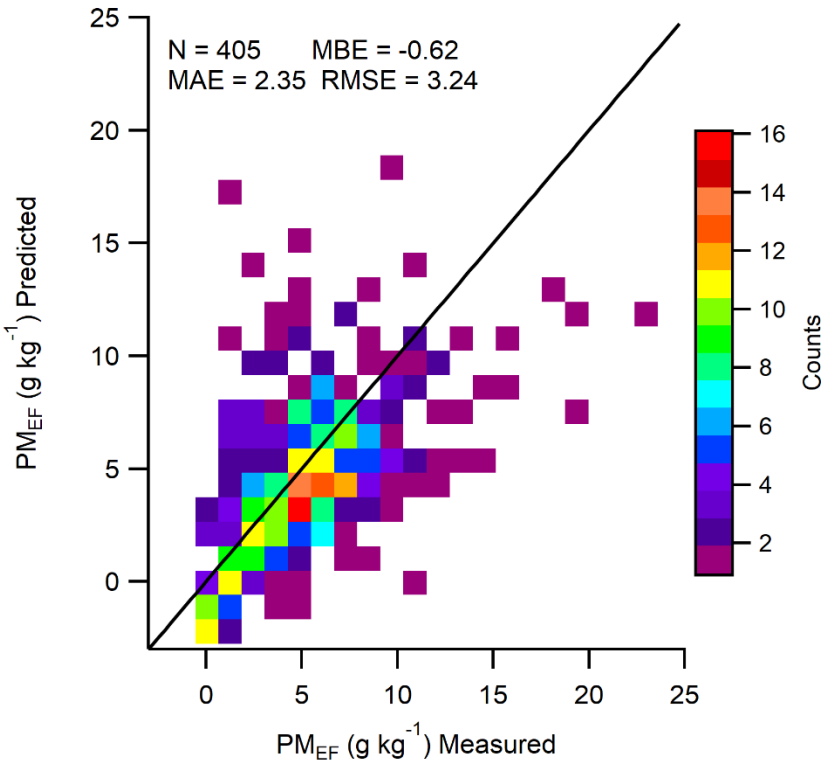

Figure S7. Scatter density plot between predicted and measured EFs of PM. The parameter N represents the number of data points, MBE is the mean bias error, MAE is the mean absolute error, and RMSE is the root mean square error between predicted and measured EFs of PM. The color bar represents the density of the data. The black solid line represents the one-to-one line.

Table S1. Emission factor (g kg^{-1}) for all fuels.

Attached as a xlsx file

Table S2. Literature value used in Figure 3 (main text).

Attached as a xlsx file

References

Barker, P. A., et al. (2020), Airborne measurements of fire emission factors for African biomass burning sampled during the MOYA campaign, *Atmospheric Chemistry and Physics*, *20*(23), 15443-15459, doi:10.5194/acp-20-15443-2020.

Eilenberg, S. R., et al. (2018), Field measurements of solid-fuel cookstove emissions from uncontrolled cooking in China, Honduras, Uganda, and India, *Atmospheric Environment*, *190*, 116-125, doi:10.1016/j.atmosenv.2018.06.041.

Grieshop, A. P., G. Jain, K. Sethuraman, and J. D. Marshall (2017), Emission factors of health- and climate-relevant pollutants measured in home during a carbon-finance-approved cookstove intervention in rural India, *Geohealth*, *1*(5), 222-236, doi:10.1002/2017GH000066.

Maricq, M. M., and N. Xu (2004), The effective density and fractal dimension of soot particles from premixed flames and motor vehicle exhaust, *Journal of Aerosol Science*, *35*(10), 1251-1274, doi:10.1016/j.jaerosci.2004.05.002.

Pokhrel, R. P., J. Gordon, M. N. Fiddler, and S. Bililign (2021), Impact of combustion conditions on physical and morphological properties of biomass burning aerosol, *Aerosol Science and Technology*, *55*(1), 80-91, doi:10.1080/02786826.2020.1822512.

Selimovic, V., R. J. Yokelson, C. Warneke, J. M. Roberts, J. de Gouw, J. Reardon, and D. W. T. Griffith (2018), Aerosol optical properties and trace gas emissions by PAX and OP-FTIR for laboratory-simulated western US wildfires during FIREX, *Atmospheric Chemistry and Physics*, *18*(4), 2929-2948, doi:10.5194/acp-18-2929-2018.

Stockwell, C. E., R. J. Yokelson, S. M. Kreidenweis, A. L. Robinson, P. J. DeMott, R. C. Sullivan, J. Reardon, K. C. Ryan, D. W. T. Griffith, and L. Stevens (2014), Trace gas emissions from combustion of peat, crop residue, domestic biofuels, grasses, and other fuels: configuration and Fourier transform infrared (FTIR) component of the fourth Fire Lab at Missoula Experiment (FLAME-4), *Atmospheric Chemistry and Physics*, *14*(18), 9727-9754, doi:10.5194/acp-14-9727-2014.